

Theoretical study of the degradation of Amoxicillin by interaction with the hydroxyl radical ($\cdot\text{OH}$)

Rida Masmoudi^a, Sami Khettaf^a, Chaimaa Kahlat^a, Ammar Dibi^a, Saad Bouchekioua^b and Tahani-achouak Chinar^c

^aLaboratory of Chemistry and Environmental Chemistry, Department of Chemistry, Faculty of Material Sciences, University Of Batna 1, Batna 05000, Algeria.

^bPharmaceutical Sciences Research Center (CRSP), Constantine 25000, Algeria.

^cDepartment of physical chemistry of inorganic materials, Faculty of chemistry, USTHB University of Science and Technology, Bab Ezzouar Algiers 16000, Algeria.

*Corresponding author, email: redhachem@yahoo.fr

Received date: May 11, 2021 ; revised date: June 09, 2021 ; accepted date: June 13, 2021

Abstract

β -Lactam antibiotics are commonly used to avoid disease in humans, and antibiotics that have been excreted in the environment have caused significant concerns. Amoxicillin belongs to the penicillin, which is the most widely, consumed antibiotics that have resistance to conventional biological water treatment methods. The highest functional richness of this molecule makes it very difficult to establish the AMX degradation pathway. A better alternative to removing these toxic and recalcitrant compounds from wastewater effluents and causing their mineralization will be advanced oxidation processes (AOPs). They have emerged as a promising form of technology for pollutant degradation, converting them into safe products like CO_2 and H_2O . They're oxidative processes based on the generation of highly oxidizing species like hydroxyl radicals.

Our study uses functional density theory (DFT) to clarify the mechanisms of reactions between ($\text{OH}\cdot$) and AMX. This interaction is done either by the abstraction of hydrogen or the addition of the radical hydroxyl on the molecule; the results reveal that the addition of radicals ($\text{OH}\cdot$) that produce intermediates (add) is kinetically and thermodynamically favoured over the intermediate structures (abs) that are resulted from the abstraction of hydrogen.

Thus, the PkcsM server used to follows the toxicity study, which showed that amoxicillin/ion amoxicillin and their by-products. Could disrupt normal liver function and induce liver damage, they're toxic to the aqueous environment, where the AMX/ion AMX and their by-products obtained by the abstraction of an H are less toxic to Minnow fish than those obtained by the addition of OH (2.6 log mM), (3.9 log mM), respectively.

Keywords: amoxicillin; Degradation; Toxicity; Mechanism; DFT; Hydroxyl radical; Sonolyse.

1. Introduction

In recent decades, the term "emerging pollutants" has been broadly used to allude to a range of chemical compounds without regulatory status in the environment and its effect on human health and the environment is poorly understood [1]. the danger related to the presence of those pollutants in the environment isn't only because of their acute toxicity, but also to their genotoxicity. Their ability to develop resistance in pathogens, and therefore the risk of endocrine changes because of continued exposure of aquatic organisms to those contaminants [2]. On the opposite hand, these products designed to be biologically active can significantly affect fish and aquatic plants, even at very low concentrations [3], In the emerging pollutants category, antibiotics are one among the foremost important groups [1].

Current studies have shown that in aquatic environments, levels of antibiotics range from $\text{ng}\cdot\text{L}^{-1}$ to $\mu\text{g}\cdot\text{L}^{-1}$ within the United States., Canada, Germany, and China. Amoxicillin (AMX) (Figure 1), a broad-spectrum antibiotic aminopenicillin, which has been widely used as a sort of veterinary antibiotic in aquaculture, breeding also human medicine. Terribly, AMX has been found in a specific amount within the aquatic environment that threatens human health. The concentration of AMX was reported to be approximately $0.6\ \mu\text{g}\cdot\text{L}^{-1}$ in the British Rivers, moreover as $13\ \text{ng}\cdot\text{L}^{-1}$ at a municipal plant of wastewater treatment in Italy [4]. Because of its antibacterial nature and toxicity, AMX AMX is immune to conventional biological water treatment methods. It's, therefore, necessary to develop effective treatment techniques to stop it from entering the aquatic environment [4;5] In essence, establishing the route of degradation of AMX is harder than in other cases like paracetamol. Due to the highest functional richness of this molecule, this suggests that several oxidation pathways can form, and thus many intermediates can form. Although the kind of

treatment used can influence degradation mechanisms, previous studies have reported various routes of degradation of AMX [6].

Numerous studies are conducted on the assessment and monitoring of micropollutants and by-products in plants of wastewater treatment.

Given the increased production and consumption of emerging contaminants, like drugs, personal care products, and plasticizers [1] Agriculture, veterinary practices, and fish farming, where they're inevitably excreted within the environment [7], there's a necessity for studies that support the progress of laws and regulations that promote the environmentally sustainable use of sludge and effluent [1].

Unfortunately, conventional wastewater treatment technologies can't quantitatively eliminate these largely non-biodegradable species. As a result, new technologies are being utilized to eliminate antibiotics from wastewater [7]. These include photochemical mineralization [8] Photocatalytic degradation by Fenton and Fenton-integrated [9] hybrid oxidation processes, photo-Fenton by the solar process [6]; O₃/Fenton process [10]. Removal by Auto-Engineered Sulphonated Polyether Membrane using Nano Filtration [11]; Synthesis of Nano-composite hydrogel poly (methacrylic acid) / montmorillonite for effective absorption of amoxicillin in the aqueous medium [12]. Elimination of amoxicillin from wastewater using organobentonite [13]. Oxidative degradation of amoxicillin [by heat-activated persulphate (PAT) [14;15]. And UV-activated persulphate [16]. By adsorption [17;18]. Electrochemical degradation [19]. From an aqueous solution by a multi-wall carbon nanotube filter [20]. Degradation by anaerobic degradation systems [21]. Ultrasound [22], and medium- and high-frequency ozone based on advanced oxidation [23], treatment by advanced oxidation process [24;22;5;25].

The choice of the most efficient wastewater treatment with the above criteria depends on its later purpose. Attention should be paid to adding applied chemical processes and the residual products arising from the treatment process. This avoids contamination and salting problems related to freshwater sources. Therefore, processes of decontamination and disinfection of wastewater that are cheaper, more robust, and more practical are necessary without hurting human health or stressing the environment due to treatment itself, particularly in sub-developed. during this context, advanced oxidation processes (POAs) are considered to be a successful water treatment technology for the elimination of organic contaminants known as bio-recalcitrants (persistent organic contaminants) and for the inactivation of non-treated pathogenic microorganisms through traditional techniques [25]. They're oxidative processes supported the generation of highly oxidizing species like hydroxyl radicals (HO \cdot). the primary characteristics of this species are its high reduction potential and its non-selective nature within the elimination of toxic and chronic compounds present in natural waters or wastewater that are treated using

conventional technologies [26;27]. Hydroxyl radicals are optimal within the strong oxidizer group because they meet a series of requirements [5].

- Don't create additional waste.
- they're non-toxic and have a short lifespan
- They're not corrosive to equipment parts.
- they're usually produced by simple to handle assemblies

Experimental studies of this degradation take months and years and are the results of by-products that are difficult to separate and cost little to separate, for this reason; we are going to monitor this degradation by quantum methods that are cheaper and faster and provide more accurate results. To assess their toxicity levels.

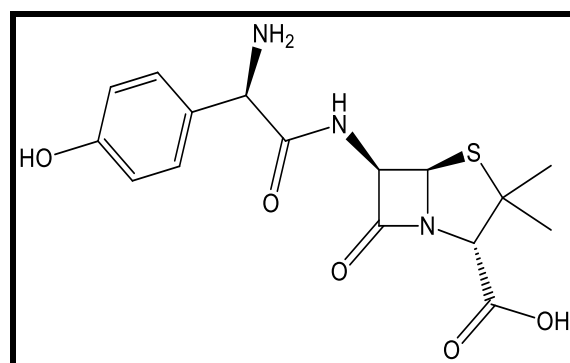


Figure 1. molecular structure of amoxicillin

2. Computational methodology

Most of the theoretical studies that were done on organic compounds further as amoxicillin used the calculation level (DFT/B3LYP) with functional 6-31 G (d) or 6-311 G (d) [28-30], Functional density theory (DFT) is now a well-established tool for tackling the quantum mechanics of the many-body systems. Originally used to calculate the properties of atoms and simple molecules, it is more complicated in chemical sciences [31]; The B3LYP the foremost popular functional DFT to date [32] it had been introduced by the Becke team in 1993 [33], The particularity of this function is to present a linear combination between GGA correlation and Hartree-Fock exchange functions. The exchange energy calculated by this method consists of 80% DFT and 20% HF [34], B3LYP is applied in structural studies of molecules with aromatic side chains [28]. The Conductive Polarized Continuum Model (CPCM) is one of the most effective solvation models that use multiple cavity models. Is applied to calculate aqueous solvency free energies for a variety of organic molecules (30 neutral molecules, 21 anions, and 19 cations); CPCM provides free energies of aqueous salvation according to experimental data and with improved computing times compared to other cavity methods [35;36].

Structural parameters (bond lengths and bond angles) and spectroscopic studies (IR) provide a basis for clarifying the structure of Chemical species. In this study, the studied

compound is optimized at DFT/B3LYP/6-31G+ (d) level in both the gas and water phases using the model CPCM, where water ($\epsilon = 78.36$) was used as a solvent.

2.1. Computational Details

The compounds studied were drawn with GaussView 6.0.16; allows the user to perform Gaussian calculations from a graphical interface without the necessity to use instruction, and helps interpret the Gaussian output [37]; therefore the calculation was performed via Gaussian16. The calculation includes density functional theory (DFT) [31]; hybrid B3LYP [32], and is utilized for the essential set of 6-31G+ (d). Optimized molecular geometry using B3LYP / 6-31G (d) levels within the gas and solvate phases; the IR spectrum was obtained from optimized structures. Electronic chemical potential μ ; Chemical hardness η (energy gap) and softness S [29].

$$\mu \approx (E_{\text{HOMO}} + E_{\text{LUMO}}) / 2 \quad (1)$$

$$\eta \approx (E_{\text{HOMO}} - E_{\text{LUMO}}) / 2 \quad (2)$$

$$S = 1 / \eta \quad (3)$$

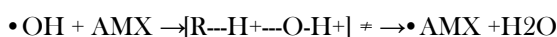
$$\omega = \mu^2 / 2\eta \quad (4)$$

$$N = -Is \quad (5)$$

Electrophilicity ω and Solution phase ionization potential, Is

The stability of the radicals generated as a result of H abstraction and OH addition was calculated using Eq (6), Eq (7), Eq (8) and Eq (9) [22;38].

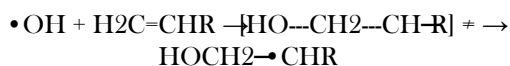
Abstraction



$$\Delta_r H_{(298\text{K})}^\circ = \Delta_f H_{\text{AMX}}^\circ(298\text{K}) + \Delta_f H_{\text{H}_2\text{O}}^\circ(298\text{K}) - \Delta_f H_{\text{AMX}}^\circ(298\text{K}) \quad (6)$$

$$\Delta_r G_{(298\text{K})}^\circ = \Delta_f G_{\text{AMX}}^\circ(298\text{K}) + \Delta_f G_{\text{H}_2\text{O}}^\circ(298\text{K}) - \Delta_f G_{\text{AMX}}^\circ(298\text{K}) \quad (7)$$

Addition



$$\Delta_r H_{(298\text{K})}^\circ = \Delta_f H_{\text{AMX}}^\circ(298\text{K}) - \Delta_f H_{\text{AMX}}^\circ(298\text{K}) \quad (8)$$

$$\Delta_r G_{(298\text{K})}^\circ = \Delta_f G_{\text{AMX}}^\circ(298\text{K}) - \Delta_f G_{\text{AMX}}^\circ(298\text{K}) \quad (9)$$

The Fukui Condensed Index representing the attack of atomic free radicals (f^0) on AMX was utilized to calculate the attack sites of free radical to search out the foremost possible fragmentation sites on AMX/AMX-. The Fukui indices were calculated by Eq (12) [29;39].

$$f^+(r) \approx \rho_{\text{N}+1}(r) - \rho_{\text{N}_0}(r) \quad (10)$$

$$f^-(r) \approx \rho_{\text{N}_0}(r) - \rho_{\text{N}-1}(r) \quad (11)$$

$$f^0(r) \approx \rho_{\text{N}+1}(r) - \rho_{\text{N}-1}(r) \quad (12)$$

The dipolar moment is that the magnitude that expresses the polarity of a molecule, A +q point charge separated from an equal and opposite point load -q by a distance d is an electrical dipole. an electrical dipole includes a moment p" which may be a vector of magnitude J.L = qd, which is meant to act within the direction of +q to -q [40]. The highest occupied energy molecular orbit (HOMO) (filled or partially filled), and also the unoccupied low energy molecular orbital (LUMO) (completely or partially vacant) of a molecular entity, Examining the mixture of molecular orbitals borders reactive molecular entities allow an approach to the interpretation of reaction behavior, this simplifies the disruption of the molecular orbital theory of chemical behavior [41], The electrostatic potential is such a powerful tool that has provided information on the intermolecular association and molecular properties of small molecules [42], it's the foremost useful electrostatic property for studying the connection between structure and activity [43].

2.2. The Toxicity Study

In 1962, Hansch et al. paved the way for the event of quantitative structure-property and structure-activity relationships (QSAR and QSPR, respectively) by correlating physicochemical properties with biological activity; this fundamental study is named Hansch's analysis [44;45] (QSAR) and (QSPR) methods are important. The drug discovery facility; has probably been one of the original industries to understand, QSPR/QSAR technology and continues to be its largest user [46;47]. To attain a more stable and reliable drug registration system, the so-called ADMET (absorption, distribution, metabolic excretion, and toxicity) design was developed and suggested.

In recent years, in silico ADMET, studies became more important, as these techniques should reduce the danger of late failure of drug development and thus allow working with only a couple of promising compounds. the event and application of those silica calculation methods have reduced the price and time of drug discovery, which is of general interest [48-50].

2.3. ADMET prediction

Regarding ADMET predictions, there are several Web Tools associated with ADMET prediction, but many researchers have used the foremost developed server pkCSM [51], to predict the properties of silico ADMET [48;50;52], For this reason, it'll be the server utilized in this study.

2.4. PkcsM (Predicting Small-Molecule Pharmacokinetic)

Drug development features a high rate, and poor pharmacokinetics and safety properties are a big barrier. Computer approaches can help reduce these risks. They developed a replacement approach (pkCSM) that uses graphical signatures to build predictive ADMET models, central properties for drug development. PkCSM works additionally or better than current methods. A freely accessible web server (<http://biosig.unimelb.edu.au/pkcsM/>), which doesn't store any information submitted to it, provides an integrated platform for rapidly assessing pharmacokinetic and toxic properties [51].

2.5. Toxicity

Toxicity is the extent to which the substance can damage the organism or the substructure of the organism, like cells and organs, and remains one of the most important reasons. For late-stage drug development failure Mechanisms of toxicity are categorized as structure-related toxicity (structural and physicochemical properties allowing interactions at sites become independent from the target) pharmacophoric-induced toxicity (e.g., human ether-a-go gene binding), metabolism-induced toxicity (e.g., electrophiles may react with nucleophilic functions in endogenous biomolecules and cause organ toxicity) and dosage-related toxicity (monitored by experimental methods like the "maximum tolerated dose" (MTD), or the oral dose in rats (LD₅₀) [52].

2.6. The Ames test

The Ames test is the most commonly used in vitro genotoxicity test [53]; compounds that are expected to be positive within the Ames test may cause mutagenicity [49].

2.7. Maximum Tolerated Dose

The maximum dose of treatment or a drug that doesn't cause undesirable side effects, the most tolerated dose is set in clinical trials by increasing doses in numerous groups of people until the highest dose with acceptable side effects is found. Also referred to as BAT [54].

2.8. HERG (human ether-a-go-go-related gene)

Several kinds of cardiovascular toxicity problems have to be considered, but, indeed, the promiscuous block of the human heart gene linked to ether-a-go-go (hERG) the channels of a spread of structurally different low molecular mass drugs represent a serious Therapeutic challenge with a profound effect on human health [52]. The recommended range for a perfect drug should be -5 and above, as a worth below this level should cause cardiac toxicity [49].

2.9. Oral Rat pLD₅₀

The median lethal dose (LD₅₀), is a standard measure of acute toxicity (dose that kills 50% of treated animals when administered over a given period) used to determine the relative toxicity of various molecules. Acute toxicity explains the adverse effects of a substance that occur within a short period after exposure and is an important indicator of drug safety assessment typically performed in the early stages of studies toxicology of unknown substances [52].

2.10. chronic oral toxicity

Chronic toxicity is described as the adverse effects that occur after repeated or continuous administration of a test sample for a large part of the service life [55;56].

2.11. Hepatotoxicity

Hepatotoxicity Considered one of the essential reasons for drug withdrawal from pharmaceutical development and clinical use [52], This parameter predicts whether a compound could interfere with normal liver function or not. A compound is defined as hepatotoxic when at least one pathological or physiological liver event related to its function is identified [49].

2.12. *Tetrahymena pyriformis*

Is an aquatic animal (Protozoan) that lives in freshwater. It is pear-shaped, 50 x 30 pm long, multiplies in 3-4 hour, and can be grown in a sterile single-link crop [57].

2.13. *Tetrahymena pyriformis*

Fathead Minnow (fat Head minnow, Pimephales promelas), is a species of temperate freshwater fish belonging to the genus Pimephales, family Cyprinidae (order Cypriniformes) [58]. Found in ponds, lakes, and mud-bottomed streams in North America and south-eastern Europe. Somewhat similar fish with rounded tails and snouts, minnows are characterized by deep, compressed bodies, usually five to eight centimeters long, and a short, flattened head on the back with a blunt snout, round side-eyes, and an inverted terminal mouth [59]. They often bury their tails first in the mud; they can survive in water too low in oxygen to support other fish [60] The attributes of the Fathead Minnow also make it an excellent model to address new challenges in aquatic toxicology [61].

3. Results and discussion

3.1. Initial reaction of amoxicillin with •OH

Amoxicillin is a semi-synthetic antibiotic [1] belonging to the β -lactam penicillin group, with a wide range of action. This class of antibiotics works by disrupting the cell walls of

bacteria during reproduction [62]. Generally used since the early 1980s in the treatment of broncho-pulmonary, pleural, and ENT infections [Amoxicillin and Clavulanic Acid]. It is included in the WHO list of essential medicines. Its availability, therefore, constitutes a major challenge for the treatment of patients in the pathologies of bacterial infections with sensitive germs [63]. One of the preconditions for the biological activity of a molecule is that it must be able to pass through the cytoplasmic membranes of different cells between its site of administration and its site of action. Amoxicillin is an amphoteric molecule. the PKa values of these proton donor groups (-COOH and -OH) and proton receptor groups (-NH₂) are 2,4, 9,6, and 7,4 [64] or (. 2.67, 9.55 and 7.11) [65]. Or (2.68; 8.49 and 7.49) [17].

Amoxicillin can produce toxic effects on microorganisms [66], aquatic organisms [11] at various trophic levels and produce an ecological imbalance. Amoxicillin can bio-accumulate within the muscle tissues of fish. with the Possibility of the presence of those drugs in food, resulting in passive consumption of this antibiotic leading to adverse effects on consumer health like immunoallergic responses [1].

A better process to eliminating these toxic and recalcitrant compounds from wastewater effluents and causing their mineralization could be advanced oxidation (AOP) processes [22-25] which are based on the chemical,

photochemical or photocatalytic production of hydroxyl radicals (HO•), which act as powerful oxidizers. The AOP has emerged as a promising form of technology for the degradation of pollutants, as they convert them into harmless final products such as CO₂ and H₂O [67;22;5].

The AOP destroys the organic molecules, even the foremost stable and difficult to degrade. Including carcinogens and mutagens, using the generation of highly reactive species that oxidize organic matter; As a result.

The AOP may be of great interest to public health and switch into a promising field of study because of its potential for pretty much total degradation of organic contaminants in water and soil, a number of them in an exceedingly reasonably gentle temperature and pressure condition [68]. In an aqueous medium, •OH can either abstract or add to hydrogen from it to supply either abstraction or addition intermediates, respectively.

In Figures 2 and 3, the reaction sites of AMX are labeled with numbers (4, 5, 6, 7, 9, 10, 17, 20, 27, 28, 29, 33, and 38) to characterize their reactivity upon H abstraction and OH addition reactions. •OH can abstract hydrogen from the aromatic (5, 9, 10, 29, 33) or β-lactam position (38), resulting in the formation of a radical carbon center on the AMX molecule also the elimination of water (Figure 2).

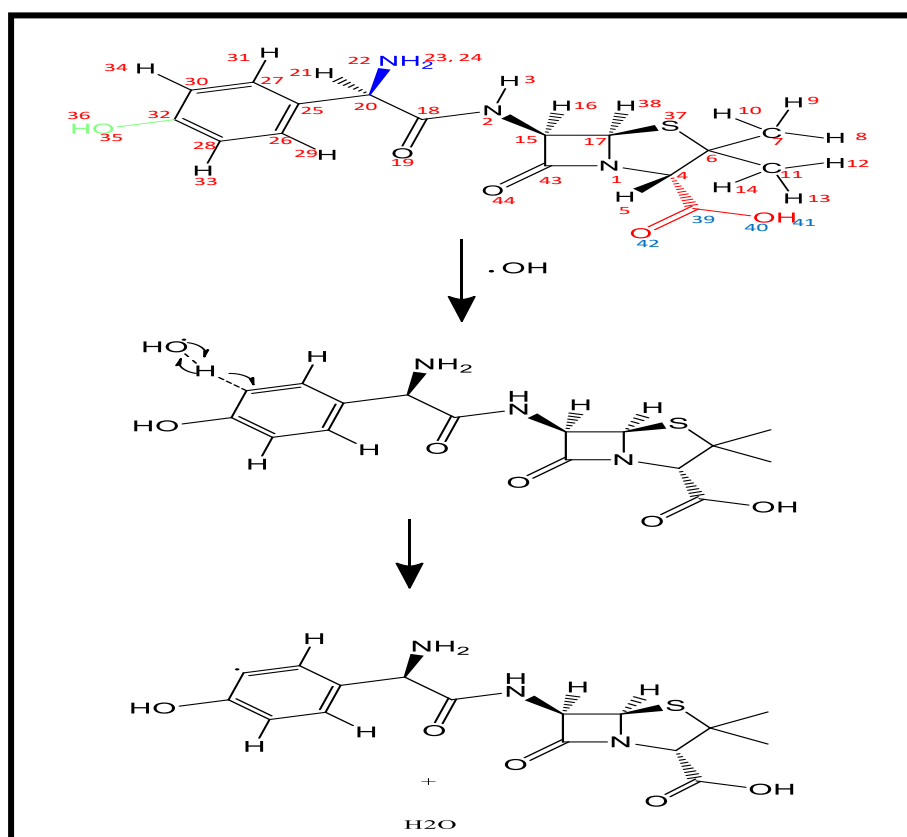


Figure 2. In aqueous medium, •OH can readily add to aromatic molecules producing hydroxycyclohexadienyl-type radicals [22] Hence, •OH could add to AMX forming AMXadd intermediates as shown in Figure 3

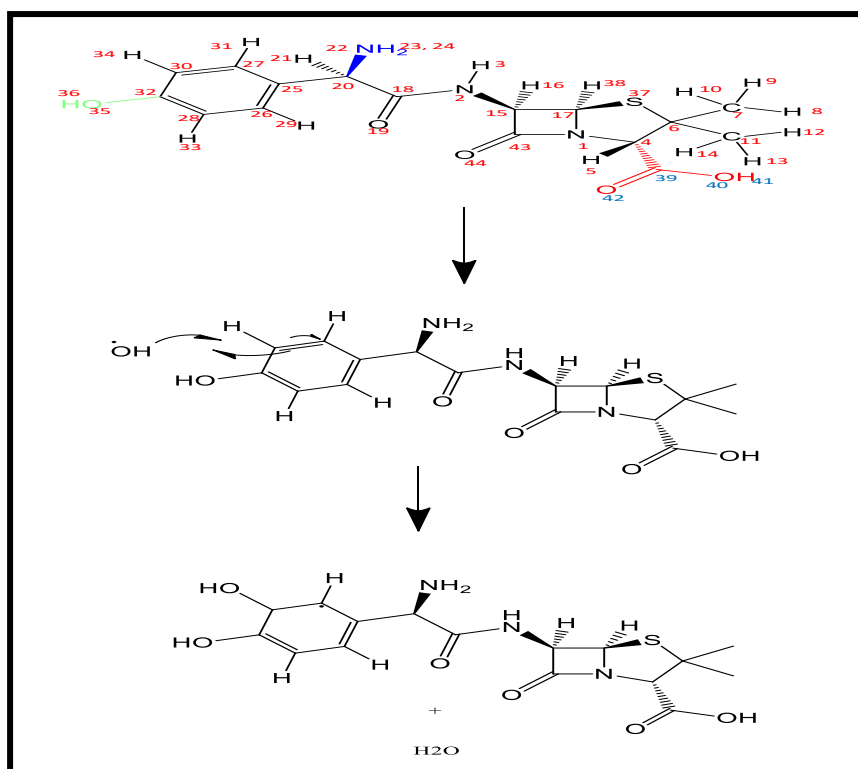


Figure 3. The Fukui Condensed Index representing the attack of atomic free radicals (f_0) on AMX was used to calculate the attack sites of free radicals [39].

These are the results of the following tables (Table 1), (Table 2). It has been found that the sites which will undergo a radical attack (abstraction of H^+ /addition of $\bullet OH$) are the carbon atoms and hydrogen atoms in the ortho position of the part bounded to C25 and of the hydroxyl group (O35 H36) and on the nitrogen atom N2. These atoms participate in an electronic delocalization

(unsaturated bonds) also, the addition to the carbon of β -lactam and thiazolidine heterocyclic cycle, these heterocyclics are unstable.

This means that the radical attack can take place on atoms that participate in an electronic conjugation, or on the sites of unstable heterocyclic.

Table 1: Fukui functions and hydroxyl radical attack sites of amoxicillin

Amoxicillin		
Isolated state		
atoms	f°	Reaction
N2	0,028	• OH Addition
C4	0,346	• OH Addition
C6	0,054	• OH Addition
H10	0,003	H+ Abstraction
C17	0,358	• OH Addition
C20	0,016	• OH Addition
C26	0,446	• OH Addition
C27	0,098	• OH Addition
H29	0,010	H+ Abstraction
C32	0,133	• OH Addition
Solvated state		
atoms	f°	Reaction
C4	0,273	• OH Addition
C6	0,017	• OH Addition
C11	0,033	• OH Addition
C17	0,206	• OH Addition
C26	0,096	• OH Addition
C27	0,184	• OH Addition
C32	0,087	• OH Addition
C43	0,047	• OH Addition

Table 2: Fukui functions and hydroxyl radical attack sites of ion amoxicillin

Ion amoxicillin		
Isolated state		
Atoms	f°	Reaction

3.2. IR Analysis

The results of the infrared spectral analysis showed the existence of several absorption bands at different

N1	0,095	• OH Addition
N2	0,021	• OH Addition
H5	0,002	H+ Abstraction
C6	0,359	• OH Addition
H9	0,010	H+ Abstraction
H10	0,019	H+ Abstraction
C11	0,026	• OH Addition
H12	0,005	H+ Abstraction
C17	0,103	• OH Addition
C18	0,060	• OH Addition
N22	0,147	• OH Addition
C25	3,196	• OH Addition
C27	0,975	• OH Addition
C28	2,996	• OH Addition
H33	0,022	H+ Abstraction
O35	0,265	• OH Addition
H38	0,009	H+ Abstraction
O43	0,019	• OH Addition
Ion amoxicillin		
Solvated state		
atoms	f°	Reaction
N2	0,020	• OH Addition
C4	0,002	• OH Addition
C6	0,122	• OH Addition
C15	0,500	• OH Addition
C20	0,284	• OH Addition
C28	0,036	• OH Addition
H29	0,001	H+ Abstraction
H31	0,010	H+ Abstraction
C32	0,029	• OH Addition

frequencies (ν), each frequency corresponds to a functional group. (Figure 4), (Figure 5), (Figure 6) and (Figure7).

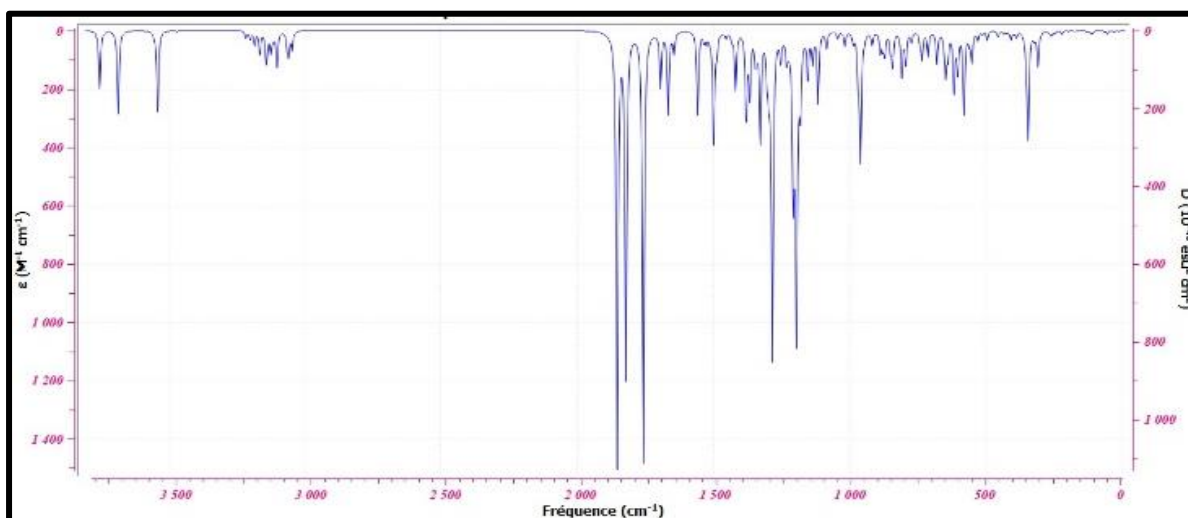


Figure 4. Theoretical IR spectra of Amoxicillin using DFT at B3LYP/6-31 + G (d) level in gas phase

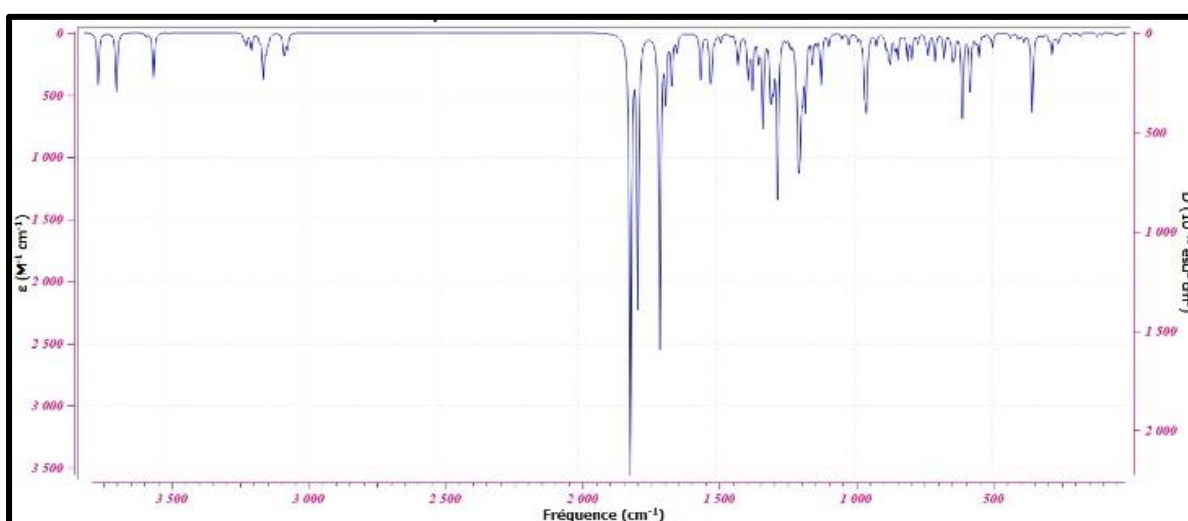


Figure 5. Theoretical IR spectra of Amoxicillin using DFT at B3LYP/6-31 + G (d) level in the solvent state

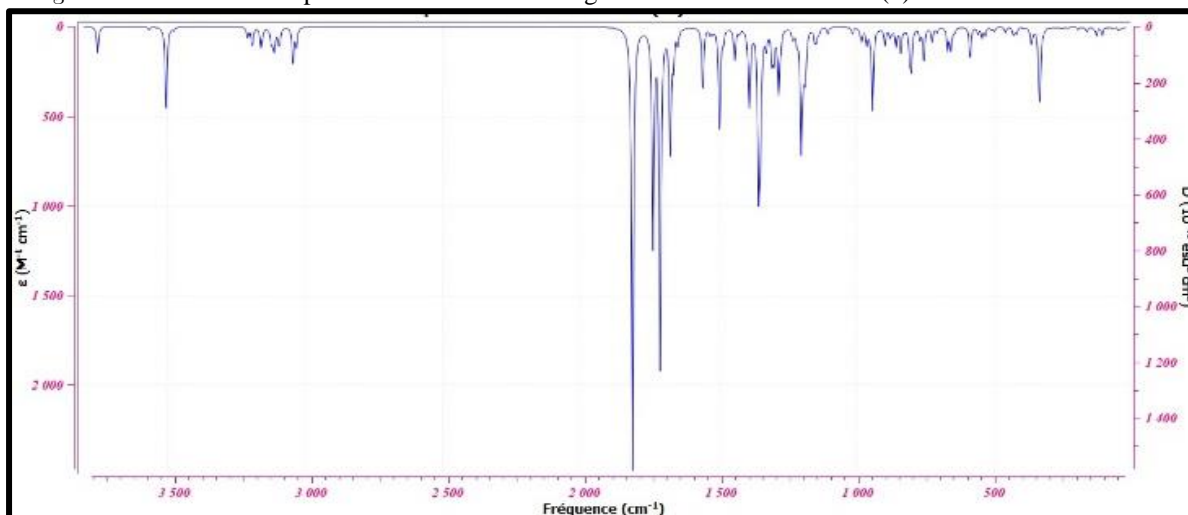


Figure 6. Theoretical IR spectra of Amoxicillin (-1) using DFT at B3LYP/6-31 + G (d) level in gas phase

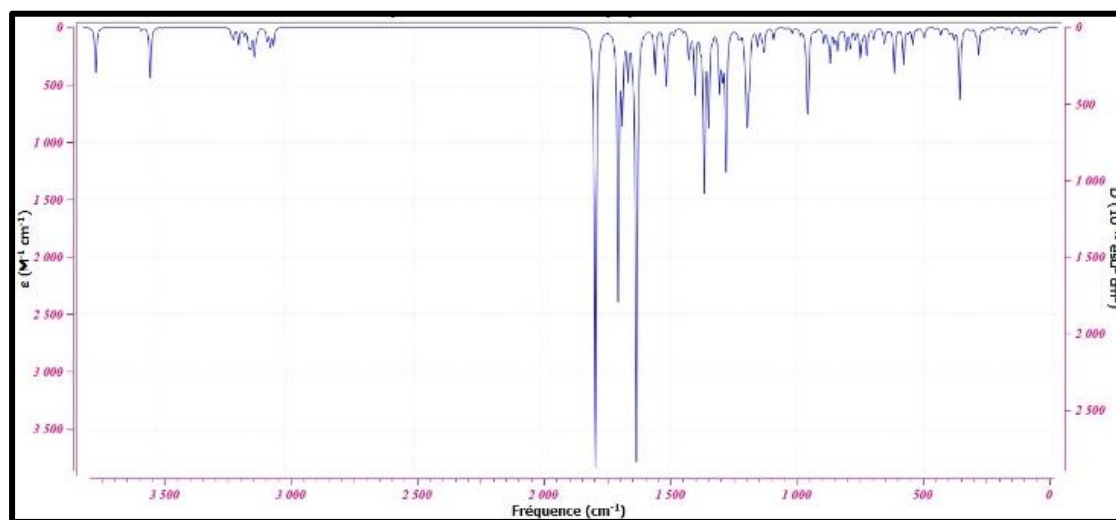


Figure 7. Theoretical IR spectra of Amoxicillin (-1) using DFT at B3LYP/6-31 + G (d) level in the solvent state

As seen in figures 4, 5, 6 and (Figure 7) it was observed that the characteristic bands of the aromatic nucleus, the carbonyl of the acid, and the secondary and tertiary amides, were moved to different wavelengths according to a bathochromic or hypochromic effect, and different intensities depending on a hypochromic or hyperchromic effect.

First, by comparing the absorption bands of the carboxylate groups of secondary amides between the isolated state and the solvated state, it was found that there is a bathochromic effect (AMX: isolated state (1755.96 cm^{-1})-(1702.11 cm^{-1}) solvate state), (AMX -1: isolated state (1735.59 cm^{-1}) - (1697.08 cm^{-1}) solvency). Where the frequencies in the solvency state are lower than in the isolated state. It means there is a bathochromic effect.

Second, by comparing the absorption bands of the carboxylate groups of tertiary amides (beta-lactam nucleus) between the isolated state and the solvated state of the two molecules, (AMX: isolated state (1852.12 cm^{-1})-(1808.76 cm^{-1}) solvate state), (AMX -1: isolated state (1810 cm^{-1}) - (1785, 81 cm^{-1}) solvency) also there is a bathochromic effect.

Third, by comparing the absorption bands of the carboxylate acid groups between the isolated state and the solvent state, (AMX: isolated state (1820.16 cm^{-1})-(1781.86 cm^{-1}) solvent state), (AMX: isolated state (1710.17 cm^{-1}) - (1625.96 cm^{-1}) solvent state)

The bathochromic effect means that a group of atoms decreases the absorption frequencies due to substitution or a solvent effect, in our study the solvent is the only factor that has been changed.

Fourth, comparing the absorption bands of the aromatic groups (C-H) between the isolated state and the solvated state, (AMX: isolated state ($3163, 23\text{ cm}^{-1}$)-(3180, 27 cm^{-1}) solvate state), (AMX -1: isolated state ($3158, 64\text{ cm}^{-1}$) - (3180, 27 cm^{-1}) solvent state). A hypochromic effect has been found (when a chromophore increases the frequency

of absorption, due to substitution or a solvent effect is called a hypochromic effect).

Concerning the different intensities, it was observed that for the solvent absorption bands for the two molecules are slightly more intense (ϵ higher) in comparison with that in the isolated state, it indicates that there is a hyperchromic effect where the absorption intensity increased by the chromophore (a function or a group of atoms)

So when there is a polar solvent (H₂O) functions with a certain polarity undergo a bathochromic effect while apolar functions (C-H aromatic) undergo a hypochromic effect simultaneously, all functions undergo a hyperchromic effect.

So when there is a polar solvent (H₂O) the functions having a certain polarity undergo a bathochromic effect whereas apolar functions (aromatic C-H) undergo a hypochromic effect simultaneously all the functions undergo a hyperchromic effect.

Studies have been carried out at DFT/B3LYP/6-31G(d) [69;70] and DFT/B3LYP/6-311G(d) [71] in an isolated condition, confirm our results where they found the same frequencies of groups characteristic of amoxicillin [69-71].

3.3. Electronic parameters

For the values of the bond indices, it was observed when comparing the solvency by the isolated state for each molecule, that all the bonds have the same value of the bond index except for the different amoxicillin bond O40C39. This implies that the electrons are moved from the interatomic region and point to an anti-binder interaction [72] during the existence of the solvent. Besides, the bonds (C39=O40) and (C39=O41) of amoxicillin (-1) which are in the form of a salt and their value is equal to two, (Table 3).

Table 3: values of the bond indices of amoxicillin and ion amoxicillin in the isolated and solvent state

Amoxicillin			Ion amoxicillin		
Bond Å	Isolated	solvate (H.O)	Bond Å	Isolated	Solvate H.O
O40C39	1	1.5	O40C39	2	2

For the distribution of charges, the opposite atomic charges provided an attractive force [73]. (Figure 8) (Figure 9) (Figure 10) and (Figure 11), their values have been observed to differ, the reddest atoms are negatively charged and the greenest are positively charged. The blackest colored atoms, and the most purple, represent the completely neutral atoms and the least negatively charged respectively, By carefully analyzing these charge distributions, It can be seen that the partial atomic charges of amoxicillin and amoxicillin (-1) differ at the level of the aromatic side-chain;(C25, C26; C27 C28; C30), (H29; H31; H33; H34) by other words in the ortho position of the aromatic nucleus so that:

(C26; C27) are in the ortho position of the related part of C25,

(C28; C30) are in the ortho position of the hydroxyl group (O35 H36),

This means that the electron donor substitutes (O35H36 and the chain linked to C25) increase the negative charge at the ortho and para position of the aromatic nucleus. Only for AMX-1 in the isolated state C25 is charged negative because it is in the para position by contribution to the hydroxyl group (O35 H36) it means that in this case, the effect of the hydroxyl group is stronger than that of the chain bound to C25.

All dipolar moment values are positive (Figure 8) (Figure 9) (Figure 10) (Figure 11), indicating that the molecules are not plane. A large dipolar moment value for a molecule indicates that there is a van der Waal-type intermolecular interaction or a hydrogen bond; the absence of a characteristic band of a hydrogen bond (strong and wide absorption band from 3200cm^{-1} to 3400cm^{-1}) in the IR spectra, indicates that there are only van der Waals-type interactions. which explains our case were amoxicillin (-1) (isolated state 14,250 D; solvent state 22,911 D) has more intermolecular interaction than amoxicillin (isolated state: 3,538 D; solvate state 6,353 D); and at the same time each molecule in its solvate state to more intermolecular electrostatic interaction than in its isolated state, these electrostatic interactions are between two permanent multipôles. We call them Keesom's forces.

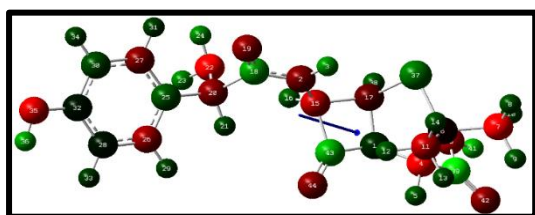


Figure 8. Distribution of atomic charge and dipole moment vector of AMX in the isolated state

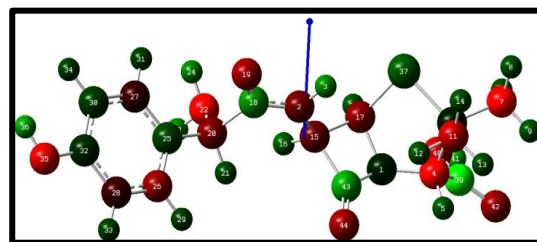


Figure 9. Distribution of atomic charge and dipole moment vector of AMX in the solvated state

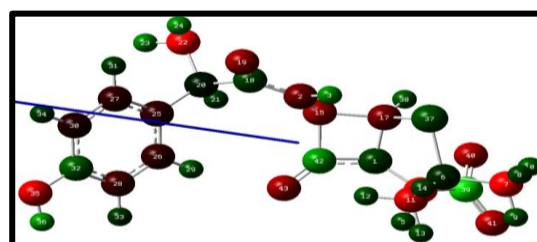


Figure 10. Distribution of atomic charge and dipole moment vector of AMX(-1) in the isolated state

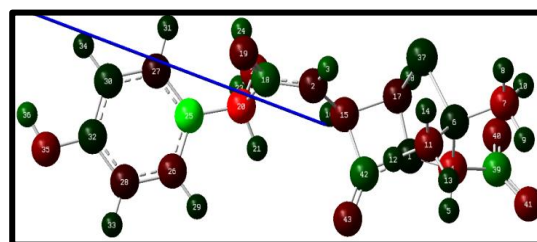


Figure 11. Distribution of atomic charge and dipole moment vector of AMX (-1) in the solvated state

3.4. Orbital analysis and description of reactivity

3.4.1. Overall hardness

The overall hardness expresses the resistance of a system to the change in its number of electrons. The molecular orbital diagrams obtained in DFT show a mean energy gap between the molecular orbitals HOMO and LUMOs (0.18722 Hartree; 0.19694 Hartree); (0.14445 Hartree; 0.20416 Hartree) of amoxicillin (isolated state, solvate), and amoxicillin (-1) (isolated state, solvency state) respectively. (See Figure 12). This reflects average stability, where it is noted that the two molecules are slightly more stable in the solvency state by contribution to the isolated state, (Figure 13), (Figure 14). through electron displacement and intermolecular electrostatic interactions.

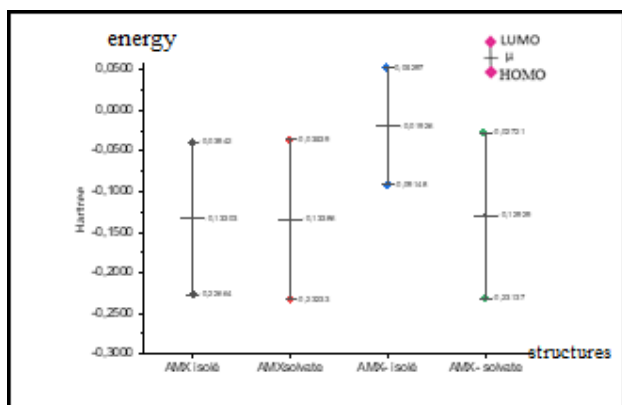


Figure 12. Energy gap of Homo-Lumo of amoxicillin molecule

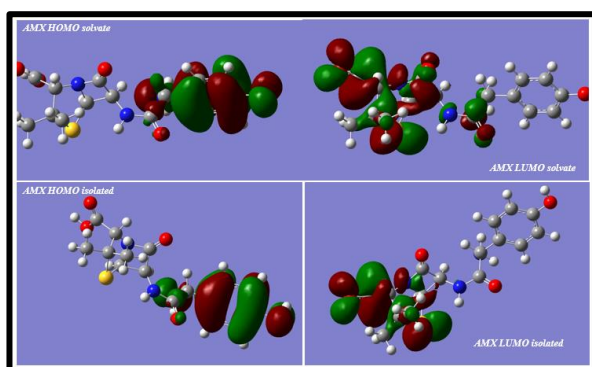


Figure 13. HOMO and LUMO density distribution in the isolated and solvent state of amoxicillin (AMX).

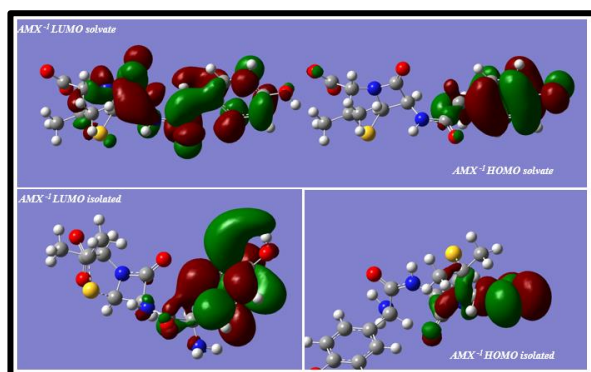


Figure 14: HOMO and LUMO density distribution in the isolated and solvent state of amoxicillin ion (AMX(-1)).

3.4.2. Electronic chemical potential (μ)

The electronic chemical potential represents the tendency of an atom or molecule to keep its electrons. Amoxicillin (-1) and amoxicillin in an isolated state (-0.01926 Hartree), (-0.13303 Hartree) respectively tend to keep their electrons higher in proportion to their solvate, (-0.12929 Hartree), (-0.13386 Hartree), (see Figure 15), this indicates that the two molecules of amoxicillin in the solvated state can give electrons.

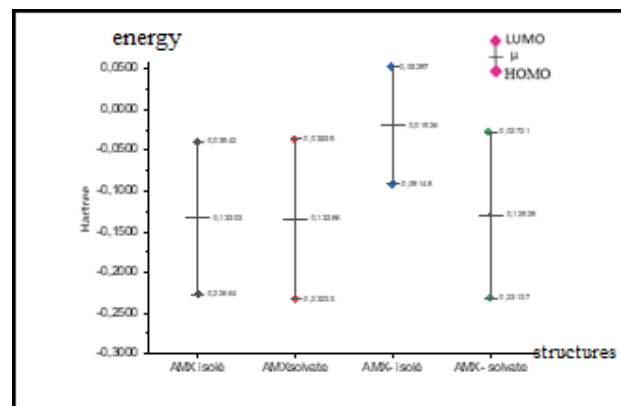


Figure 15. Energy gap of Homo-Lumo of amoxicillin ion(-1).

3.4.3. Global electrophilicity

The results show that amoxicillin in the isolated state can accept electrons relative to other states (Table 4); these results were confirmed by another study [69].

Table 4: Overall electrophilicity of amoxicillin and amoxicillin (-1)

	AMX		Ion AMX	
	Isolated state	Solvent state	Isolated state	Solvent state
Electrophilicity $\omega = \mu^2/2\eta$ (Hartree)	0,047	0,046	0,0013	0,041

3.5. Thermodynamic parameter

3.5.1. System entropy

The values of entropy show that amoxicillin is more ordered in its isolated state (171,151 cal/mol-kelvin) than in its solvate state (171,574 cal/mol-kelvin); and that amoxicillin (-1) in its isolated state (169,031 cal/mol-kelvin) is the most ordered than in its solvate state (170,096 cal/mol-kelvin), this means that the solvency disorder the molecule (Table 5).

3.5.2. Enthalpy and thermal energy

All thermal energies of amoxicillin and amoxicillin (-1) are positive, indicating that the systems will undergo an exothermic transformation (Table 5).

3.5.3. Transition states

Negative frequencies signify the instability of the molecule or the saddle on the potential energy surface. A stable molecule should have no imaginary frequencies, a transition state should have one (1st order saddle point), while more than one imaginary frequency means that it is a problem with the geometry of your molecule [74-76], our results show that there is no transition state (imaginary frequency is zero), (Table 5).

Table 5: Thermodynamic parameters of amoxicillin in the isolated and solvent state

	Amoxicillin		Amoxicillin (-1)	
	Isolated state	Solvated state	Isolated state	Solvated state
Temperature [Kelvin]	298.15	298.15	298.15	298.15
Pressure [atm]	1	1	1	1
Electronic Energy (EE)Kcal/mol	-978756,15	-978774,01	-978430,30	-978491,978
E(RB3LYP) Hartree	-1559.75	-1559.77	-1559.23	-1559.33
Dipole Moment (debye)	3.54	6.35	14.25	22.91
Imaginary Freq	0	0	0	0
E (Thermic) [kcal/mol]	232.90	232.68	224.59	224.57
Heat Capacity (Cv) [cal/mol kelvin]	91.81	91.91	90.35	90.34
Entropy (S) [Cal/mol-kelvin]	171.15	171.57	169.03	170.10
EE + Thermal Energy Correction [kcal/mol]	-978523,25	-978541,34	-978205,72	-978267,41
EE + Thermal Enthalpy Correction [kcal/mol]	-978522,66	-978540,74	-978205,12	-978266,82
EE + Thermal Free Energy Correction [kcal/mol]	-978573,68	-978591,89	-978255,52	-978317,53
Thermal Correction to Energy [kcal/mol]	232,90	232,68	224,59	224,57
Thermal Correction to Enthalpy [kcal/mol]	233,50	233,27	225,18	225,17
Thermal Correction to Free Energy [kcal/mol]	182,47	182,11	174,79	174,45

3.6. Thermodynamic parameters of abstraction and addition reactions

3.6.1. Amoxicillin and its by-products Isolated condition

Abstraction and addition reactions are irreversible transformations; spontaneous and exothermic reactions (table 6).

Table 6: Thermodynamic parameters of amoxicillin reactions

	$\Delta^{\circ}H$ (Hartree)	$\Delta^{\circ}S$ (kcal/mol)	$\Delta^{\circ}G$ (Hartree)	ΔrH Interpretation	ΔrS Interpretation	ΔrG Interpretation
AMX	-1559,37	171,15	-1559,46			
addC4	-1635,13	193,60	-1635,22	-75,75	22,45	-75,77
add C6	-1635,12	179,90	-1635,20	-75,74	8,75	-75,75
add C17	-1635,17	180,18	-1635,25	-75,80	9,03	-75,80
add C20	-1635,07	188,73	-1635,18	-75,71	17,58	-75,72
add N2	-1635,10	184,82	-1635,19	-75,73	13,67	-75,74
abs H10	-1558,72	174,66	-1558,80	-75,74	48,64	-75,77
abs H29	-1558,70	172,59	-1558,78	-75,72	46,56	-75,75

3.6.2. Amoxicillin (-1) and its by-product Isolated condition

Abstraction and addition reactions are irreversible transformations; spontaneous and exothermic (Table 7).

Table 7: Thermodynamic parameters of the reactions of the Amoxicillin ion

	$\Delta^{\circ}H$ (Hartree)	$\Delta^{\circ}S$ (k cal/mol)	$\Delta^{\circ}G$ (Hartree)	ΔrH interpretation	ΔrS interpretation	ΔrG interpretation
AMX (-1)	-1558,87	169,03	-1558,95			
add C6	-1634,61	182,53	-1634,70	-75,74	13,50	-75,75
add C17	-1634,66	182,96	-1634,74	-75,79	13,92	-75,79
add C27	-1634,62	175,86	-1634,71	-75,75	6,83	-75,76
add C28	-1634,61	177,20	-1634,70	-75,74	8,17	-75,75
add N2	-1634,60	183,44	-1634,69	-75,74	14,41	-75,74
abs H5	-1558,23	173,47	-1558,31	-75,76	47,44	-75,27
abs H9	-1558,21	172,42	-1558,30	-75,74	6,39	-75,26
abs H33	-1558,19	169,85	-1558,28	-75,72	43,83	-75,24
abs H38	-1558,22	172,46	-1558,30	-75,75	46,43	-75,27

3.7. Toxicity Study

A drug becomes toxic when its plasma level is higher than that needed for therapeutic effects. Hepatic, cardiac, genotoxic, mutagenic, carcinogenic (tumorigenic), reproductive, and phytochemical irritant effects were tested to identify safer molecules for therapeutic action [49].

3.7.1. The Ames test

The results showed that. AMX, AMX (-1), and their by-products do not exhibit genotoxicity.

3.7.2. HERG (cardiac toxicity)

The results show that amoxicillin and amoxicillin (-1) as well as their by-products have no cardiac toxicity.

3.7.3. Hepatotoxicity

PkcsM server forecasts suggest that the products studied induce liver damage.

3.7.4. Oral Rat pLD50

When calculating this property with the pkCSM server we note a small increase in the average pLD50 for AMX. And their abstraction by-products, abs H29/H31; abs H10 with one (LD50) equal to (2.108;2.108;2.111) (mol/kg) and

AMX (-1); AMX(-1) abs (H5); abs H12/ H10/H9;abs (H33) ; abs (H38); abs (H29/H31) solvate; with one (LD50) equal to (2.125;2.116;2.117;2.125;2.121;2.116) respectively. Compare to the other sets of by-products obtained by the addition of an OH.

3.7.5. Chronic oral toxicity

The results show that the structures studied have low chronic oral toxicity.

3.7.6. Hepatotoxicity

Amoxicillin and amoxicillin (-1) and their by-products may interfere with normal liver function.

3.7.7. Skin sensitivity

Calculated products have no skin sensitivity.

3.7.8. Aquatic toxicity (Toxicity on Minnow in (log mM), on Tetrahymena pyriformis in (log ug/L))

All structures studied are of low toxicity to the aquatic environment with toxicity to Tetrahymena pyriformis equal to 0.285 (log ug/L) and shiner fish of varying values from 2.223 to 3.314 (log mM) for amoxicillin and its by-products; and 2.6 (log mM) for amoxicillin (-1) and its by-products.

3.7.9. Observations

The β -lactam cycle opening radicals (addition to C6) are less toxic than obtained by thiazolidine cycle opening (addition to C17).

The by-products obtained by addition are slightly less toxic than obtained by the abstraction of an H[•] (Table 8) (Table 9).

Table 8: ADMET Properties of amoxicillin and its by-products

		AMX	Abs H10	Abs H29/H31	Add C4	add C6	Add C17	Add C20
Property	Model Name Unit	Predicted Value						
Absorption	Water solubility Numeric (logmol/L)	-2.882	-2.879	-2.879	-2.706	-2.929	-2.91	-2.964
Absorption	Caco2 permeability Numeric (log Papp in 10 ⁻⁶ cm/s)	-0.169	-0.162	-0.162	-0.568	-0.532	-0.488	-0.396
Absorption	Intestinal absorption (human) Numeric (% Absorbed)	39.94	39.112	39.05	22.698	30.606	23.708	32.367
Absorption	Skin Permeability Numeric (log Kp)	-2.735	-2.735	-2.735	-2.735	-2.735	-2.735	-2.735
Absorption	P-glycoprotein substrate Categorical (Yes/No)	Yes	Yes	Yes	Yes	Yes	Yes	Yes
Absorption	P-glycoprotein I inhibitor Categorical (Yes/No)	No	No	No	No	No	No	No
Absorption	P-glycoprotein II inhibitor Categorical (Yes/No)	No	No	No	No	No	No	No
Distribution	VD _{ss} (human) Numeric (log L/kg)	-0.853	-0.857	-0.857	-0.854	-1.322	-0.958	-0.644
Distribution	Fraction unbound (human) Numeric (Fu)	0.545	0.549	0.549	0.632	0.584	0.564	0.506
Distribution	BBB permeability Numeric (log BB)	-1.486	-1.46	-1.458	-1.698	-1.902	-1.658	-1.73
Distribution	CNS permeability Numeric (log PS)	-3.57	-3.574	-3.574	-3.686	-4.024	-3.995	-4.035
Metabolism	CYP2D6 substrate Categorical (Yes/No)	Yes	Yes	Yes	Yes	Yes	No	Yes
Metabolism	CYP3A4 substrate Categorical (Yes/No)	No	No	No	No	No	No	No
Metabolism	CYP1A2 inhibitor Categorical (Yes/No)	No	No	No	No	No	No	No
Metabolism	CYP2C19 inhibitor Categorical (Yes/No)	No	No	No	No	No	No	No
Metabolism	CYP2C9 inhibitor Categorical (Yes/No)	No	No	No	No	No	No	No
Metabolism	CYP2D6 inhibitor Categorical (Yes/No)	No	No	No	No	No	No	No
Metabolism	CYP3A4 inhibitor Categorical (Yes/No)	No	No	No	No	No	No	No
Excretion	Total Clearance Numeric (log ml/min/kg)	0.267	0.25	0.296	0.451	0.254	-0.083	0.63

Excretion	Renal OCT2 substrate Categorical (Yes/No)	No						
Toxicity	AMES toxicity Categorical (Yes/No)	No						
Toxicity	Max. tolerated dose (human) Numeric (log mg/kg/day)	0.632	0.641	0.641	0.902	1.13	1.109	0.973
Toxicity	hERG I inhibitor Categorical (Yes/No)	No						
Toxicity	hERG II inhibitor Categorical (Yes/No)	No						
Toxicity	Oral Rat Acute Toxicity (LD50) Numeric (mol/kg)	2.111	2.108	2.108	1.994	1.924	2.28	2.134
Toxicity	Oral Rat Chronic Toxicity (LOAEL) Numeric (log mg/kg/day)	1.965	1.994	1.996	2.676	2.7	1.496	1.99
Toxicity	Hepatotoxicity Categorical (Yes/No)	Yes						
Toxicity	Skin Sensitisation Categorical (Yes/No)	No						
Toxicity	<i>T.Pyiformis</i> toxicity Numeric (log ug/L)	0.285	0.285	0.285	0.285	0.285	0.285	0.285
Toxicity	Minnow toxicity Numeric (log mM)	2.555	2.602	2.605	2.223	2.96	3.314	3.291

Table 9: ADMET Properties of amoxicillin (-1) and its by-products

		AMX (-1)	AMX (-1) abs (H5)	abs H12/H10/H9	abs (H33)	abs (H38)	abs (H29/H31) solv	Add C17
Property	Model Name Unit	Predicted Value					Predicted Value	
Absorption	Water solubility Numeric (log mol/L)	-2.932	-2.939	-2.925	-2.925	-2.939	-2.925	-2.84
Absorption	Caco2 permeability Numeric (log Papp in 10 ⁻⁶ cm/s)	-0.031	-0.037	-0.023	-0.023	-0.037	-0.023	-0.519
Absorption	Intestinal absorption (human) Numeric (% Absorbed)	40.416	41.143	39.588	39.526	41.143	39.526	16.136
Absorption	Skin Permeability Numeric (log Kp)	-2.735	-2.735	-2.735	-2.735	-2.735	-2.735	-2.735
Absorption	P-glycoprotein substrate Categorical (Yes/No)	No	No	No	No	No	No	Yes
Absorption	P-glycoprotein I inhibitor Categorical (Yes/No)	No	No	No	No	No	No	No
Absorption	P-glycoprotein II inhibitor Categorical (Yes/No)	No	No	No	No	No	No	No
Distribution	VDss (human) Numeric (log L/kg)	-0.943	-0.941	-0.946	-0.946	-0.941	-0.946	-1.392
Distribution	Fraction unbound (human) Numeric (Fu)	0.574	0.569	0.579	0.579	0.569	0.579	0.561

Distribution	BBB permeability Numeric (log BB)	-1.037	-1.06	-1.011	-1.009	-1.06	-1.009	-1.863
Distribution	CNS permeability Numeric (log PS)	-3.563	-3.559	-3.568	-3.568	-3.559	-3.568	-4.352
Metabolism	CYP2D6 substrate Categorical (Yes/No)	Yes						
Metabolism	CYP3A4 substrate Categorical (Yes/No)	No						
Metabolism	CYP1A2 inhibitor Categorical (Yes/No)	No						
Metabolism	CYP2C19 inhibitor Categorical (Yes/No)	No						
Metabolism	CYP2C9 inhibitor Categorical (Yes/No)	No						
Metabolism	CYP2D6 inhibitor Categorical (Yes/No)	No						
Metabolism	CYP3A4 inhibitor Categorical (Yes/No)	No						
Excretion	Total Clearance Numeric (log ml/min/kg)	0.28	0.247	0.263	0.324	0.355	0.309	0.616
Excretion	Renal OCT2 substrate Categorical (Yes/No)	No						
Toxicity	AMES toxicity Categorical (Yes/No)	No						
Toxicity	Max. tolerated dose (human) Numeric (log mg/kg/day)	0.644	0.638	0.651	0.652	0.638	0.652	1.325
Toxicity	hERG I inhibitor Categorical (Yes/No)	No						
Toxicity	hERG II inhibitor Categorical (Yes/No)	No						
Toxicity	Oral Rat Acute Toxicity (LD50) Numeric (mol/kg)	2.121	2.125	2.117	2.116	2.125	2.116	1.98
Toxicity	Oral Rat Chronic Toxicity (LOAEL) Numeric (log mg/kg/day)	1.745	1.72	1.774	1.776	1.72	1.776	3.233
Toxicity	Hepatotoxicity Categorical (Yes/No)	Yes						
Toxicity	Skin Sensitisation Categorical (Yes/No)	No						
Toxicity	<i>T.Pyriformis</i> toxicity Numeric (log ug/L)	0.285	0.285	0.285	0.285	0.285	0.285	0.285
Toxicity	Minnow toxicity Numeric (log mM)	2.641	2.6	2.687	2.691	2.6	2.691	3.972

4. Conclusion

To study the degradation of amoxicillin/amoxicillin ion by hydroxyl radicals (advanced oxidation methods) and assess their toxicity: Computational approaches were used

to monitor this oxidation below the DFT/B3LYP-6-31 G+(d) level.

The vibrational analysis shows that polar functions are bathochromic and apolar functions are hypsochromic due to the existence of the solvent, which has increased van der Waals-type intermolecular interactions -Keesom forces.

Degradation of the molecule occurs at unsaturated sites; carbonyl α atoms, unstable ring atoms (β -lactam and thiazolidine ring) (C4, C17), and aromatic hydrogen atoms. The PkcsM server followed the toxicity study. Which showed that amoxicillin/ion amoxicillin and their

byproducts could disrupt normal liver function and induce liver injury. So they are toxic to the aquatic environment, where the AMX/ion AMX and their by-products obtained by the abstraction of an H⁺ are less toxic to the aquatic.

References

- [1] A. Elizalde-Velázquez, L.M. Gómez-Oliván, M. Galar-Martínez, H. Islas-Flores, O. Dublán-García, N. Sanjuan-Reyes, Amoxicillin in the aquatic environment, its fate and environmental risk. Environmental health risk—hazardous factors to living species, IntechOpen, London, 2016, Ch. 10.
- [2] B. Halling-Sørensen, S.N. Nielsen, P. Lanzky, F. Ingerslev, H.H. Lützhøft, S. Jørgensen, Chemosphere. 36 (1998) 357-393.
- [3] M.M. Huber, A. Göbel, A. Joss, N. Hermann, D. Löffler, C.S. Mcardell, A. Ried, H. Siegrist, T.A. Ternes, Von U. Gunten, Environmental science & technology. 39 (2005) 4290-4299.
- [4] W. Guo, Q.L. Wu, X.J. Zhou, H.O. Cao, J.S. Du, R.L. Yin, N.Q. Ren, Rsc Advances. 5 (2015) 52695-52702.
- [5] E.M. Cuerda-Correa, M.F. Alexandre-Franco, C. Fernández-González, An Overview. Water. 12 (2020) 102.
- [6] M.H. Guerra, I.O. Alberola, S.M. Rodriguez, A.A. López, A.A. Merino, A.E.C. Lopera, J.Q. Alonso, Water research. 156 (2019) 232-240.
- [7] X. Weng, W. Cai, S. Lin, Z. Chen, Applied Clay Science. 147 (2017) 137-142.
- [8] S.G. Pouloupoulos, G. Ulykbanova, C.J. Philippopoulos, Environmental Technology. (2020) 1-9.
- [9] M. Verma, A. Haritash, Journal of Environmental Chemical Engineering. 7 (2019) 102886.
- [10] M. Li, Z. Zeng, Y. Li, M. Arowo, J. Chen, H. Meng, L. Shao, Journal of environmental management. 150 (2015) 404-411.
- [11] A. Moarefian, H.A. Golestani, H. Bahmanpour, Journal of Environmental Health Science and Engineering, 12 (2014) 127.
- [12] S.A. Khan, M.F. Siddiqui, T.A. Khan, ACS Omega. 5, 6 (2020) 2843-2855.
- [13] S.X. Zha, Y. Zhou, X. Jin, Z. Chen, Journal of Environmental Management. 129 (2013) 569-576.
- [14] J. Zhao, Y. Sun, F. Wu, M. Shi, X. Liu, Journal of Chemistry. 2019 (2019) 1-10.
- [15] E. Kattel, B. Kaur, M. Trapido, N. Dulova, Environmental technology. 41 (2020) 202-210.
- [16] C.S. Zhou, J.W. Wu, L.L. Dong, B.F. Liu, D.F. Xing, S.S. Yang, X.K. Wu, Q. Wang, J.N. Fan, L.P. Feng, Journal of Hazardous Materials. 388 (2020) 122070.
- [17] J.M. Chaba, P.N. Nomngongo, Emerging Contaminants. 5 (2019) 143-149.
- [18] I. Anastopoulos, I. Pashalidis, A.G. Orfanos, I.D. Manariotis, T. Tatarchuk, L. Sellaoui, A. Bonilla-Petriciolet, A. Mittal, A. Núñez-Delgado, Journal of Environmental Management. 261 (2020) 110236.
- [19] R. Kaur, J.P. Kushwaha, N. Singh, Electrochimica Acta. 296 (2019) 856-866.
- [20] T.Y. Tan, Z.T. Zeng, G.M. Zeng, J.L. Gong, R. Xiao, P. Zhang, B. Song, W.W. Tang, X.Y. Ren, Separation and Purification Technology, 235 (2020) 116167.
- [21] R.V. Busto, J. Roberts, C. Hunter, A. Escudero, K. Helwig, L.H.G. Coelho, Ecotoxicology and Environmental Safety. 192 (2020) 110207.
- [22] M.I. Stefan, Advanced oxidation processes for water treatment: fundamentals and applications, IWA publishing, 2017.
- [23] R. Kıdak, Ş. Doğan, Ultrasonics sonochemistry. 40 (2018) 131-139.
- [24] F. Zaviska, P. Drogui, G. Mercier, J.F. Blais, Journal of Water Science. 22 (2019) 535-564.
- [25] J.A. Garrido-Cardenas, B. Esteban-García, A. Agüera, J.A. Sánchez-Pérez, F. Manzano-Agugliaro, International Journal of Environmental Research and Public Health. 17 (2020) 170.
- [26] D. Hermosilla, N. Merayo, A. Gascó, Á. Blanco, Environmental Science and Pollution Research. 22 (2015) 168-191.
- [27] J.L. Wang, L.J. Xu, Critical reviews in environmental science and technology. 42 (2012) 251-325.
- [28] D. Toroz, T. Van Mourik, Molecular Physics. 104 (2006) 559-570.
- [29] L.R. Domingo, M. Ríos-Gutiérrez, P. Pérez, Molecules. 21 (2016) 748.
- [30] D.J. Tantillo, Applied theoretical organic chemistry, World Scientific, 2018.
- [31] C. Fiolhais, F. Nogueira, M.a.L. Marques, A primer in density functional theory, Berlin; London, Springer, 2011.
- [32] N.A. Derevyanko, A.A. Ishchenko, A.V. Kulinich, Physical Chemistry Chemical Physics. 22 (2020) 2748-2762.
- [33] A.D. Becke, The Journal of chemical physics. 98 (1993) 1372-1377.
- [34] V.Z. Fock, Physik. 61 (1930) 126.
- [35] Y. Takano K. Houk, Journal of Physical Chemistry A. 108, 52 (2004) 11740-11751.
- [36] Y. Takano, K. Houk, Journal of Chemical Theory and Computation, 1, 1 (2005) 70-77.
- [37] M.J. Frisch, G.W. Trucks, H.B. Schlegel, G.E. Scuseria, M.A. Robb, J.R. Cheeseman, G. Scalmani, V. Barone, G.A. Petersson, H. Nakatsuji, X. Li, M. Caricato, A.V. Marenich, J. Bloino, B.G. Janesko, R. Gomperts, B. Mennucci, H.P. Hratchian, J.V. Ortiz, A.F. Izmaylov, J.L. Sonnenberg, F. Williams, Ding, F. Lipparini, F. Egidi, J. Goings, B. Peng, A. Petrone, T. Henderson, D. Ranasinghe, V.G. Zakrzewski, J. Gao,

- N. Rega, G. Zheng, W. Liang, M. Hada, M. Ehara, K. Toyota, R. Fukuda, J. Hasegawa, M. Ishida, T. Nakajima, Y. Honda, O. Kitao, H. Nakai, T. Vreven, K. Throssell, Jr. J.A. Montgomery, J.E. Peralta, F. Ogliaro, M.J. Bearpark, J.J. Heyd, E.N. Brothers, K.N. Kudin, V.N. Staroverov, T.A. Keith, R. Kobayashi, J. Normand, K. Raghavachari, A.P. Rendell, J.C. Burant, S.S. Iyengar, J. Tomasi, M. Cossi, J.M. Millam, M. Klene, C. Adamo, R. Cammi, J.W. Ochterski, R.L. Martin, K. Morokuma, O. Farkas, J.B. Foresman, D.J. Fox, Gaussian 16 Rev. C.01, Wallingford, CT, 2016.
- [38] J.W. Ochterski, *Thermochemistry in gaussian*. Gaussian Inc. 1 (2000) 19.
- [39] M. Dou, J. Wang, B. Gao, C. Xu, F. Yang, *Chemical Engineering Journal*. 383 (2020) 123134.
- [40] R.J. Gillespie, P.L.A. Popelier, *Chemical bonding and molecular geometry from Lewis to electron densities*, New York, Oxford University Press, 2001.
- [41] P. Muller, *Pure and Applied Chemistry*, 66 (1994) 1077-1184.
- [42] P.K. Weiner, R. Langridge, J.M. Blaney, R. Schaefer, P.A. Kollman, *Proceedings of the National Academy of Sciences*. 79 (1982) 3754-3758.
- [43] M. Monasterios, M. Escorche, M. Avendaño, *Journal of molecular structure*. 748 (2005) 49-55.
- [44] C. Hansch, P.P. Maloney, T. Fujita, R.M. Muir, *Nature*. 194 (1962) 178-180.
- [45] R. Satpathy, *Environmental Chemistry Letters*. 17 (2019) 123-128.
- [46] A.A. Toropov, A.P. Toropova, I. Raska Jr, D. Leszczynska, J. Leszczynski, *Computers in biology and medicine*. 45 (2014) 20-25.
- [47] L.L. Ferreira, A.D. Andricopulo, *ADMET modelling approaches in drug discovery*, *Drug discovery today*, 2019.
- [48] J. Dong, N.N. Wang, Z.J. Yao, L. Zhang, Y. Cheng, D. Ouyang, A.P. Lu, D.S. Cao, *Journal of cheminformatics*. 10 (2018) 29.
- [49] S. Fatima, P. Gupta, S. Sharma, A. Sharma, S.M. Agarwal, *Future Medicinal Chemistry*. 12 (2020) 69-87.
- [50] H. Hadni, M. Elhallaoui, *Heliyon*. 6 (2020) e03580.
- [51] D.E. Pires, T.L. Blundell, D.B. Ascher, *Journal of medicinal chemistry*. 58 (2015) 4066-4072.
- [52] D. Lagorce, D. Douguet, M.A. Miteva, B.O. Villoutreix, *Scientific reports*. 7 (2017) 46277.
- [53] B. Acree, *Toxicity and drug testing*, *BoD-Books on Demand*, 2012.
- [54] N. Gonzalez-Flesca, T. Menard, P. Comes, J.O. Grimalt, *Colloque scientifique et technique européen*. (1993) 17-37.
- [55] W.H. De Jong, J.W. Carraway, R.E. Geertsma, *In vivo and in vitro testing for the biological safety evaluation of biomaterials and medical devices*. In: Bertrand, Jean-Pierre (ed.) *Biocompatibility and Performance of Medical Devices*, Woodhead Publishing, 2012.
- [56] J., Tian, Y. Yi, Y. Zhao, C. Li, Y. Zhang, L. Wang, C. Pan, J. Han, G. Li, X. Li, *Journal of ethnopharmacology*. 213 (2018) 166-175.
- [57] Y. Yoshioka, Y. Ose, T. Sato, *Science of the total environment*. 43 (1985) 149-157.
- [58] L.M. Page, B.M. Burr, *A field guide to freshwater fishes: North America north of Mexico*, Houghton Mifflin Harcourt, 1991.
- [59] C. Cardot, *Techniques appliquées au traitement de l'eau: hydraulique, électrotechnique, procédés de traitement*, Ellipses, 2001.
- [60] C. Garon-Boucher, *Contribution à l'étude du devenir des produits phytosanitaires lors de l'écoulement dans les fosses: caractérisation physico-chimique et hydrodynamique*, PhD dissertation, Joseph Fourier University, 2003.
- [61] G.T. Ankley, D.L. Villeneuve, *Aquatic Toxicology*. 78 (2006) 91-102.
- [62] M.E. Matsubara, K. Helwig, C. Hunter, J. Roberts, E.L. Subtil, L.H.G. Coelho, *Ecotoxicology and Environmental Safety*. 192 (2020) 110258.
- [63] J.P. Croué, *Environmental Monitoring and Assessment*. 92 (2004) 193-207.
- [64] D. Bernier, *Étude et modélisation de la cinétique orale de l'amoxicilline chez le porcelet*, 2010.
- [65] Y.S. Al-Degs, A.H. El-Sheikh, D.M. Harb, *Jordan Journal of Pharmaceutical Sciences*. 13 (2020) 20-27.
- [66] X. Pan, C. Deng, D. Zhang, J. Wang, G. Mu, Y. Chen, *Aquatic Toxicology*. 89 (2008) 207-213.
- [67] A.F. Martins, F. Mayer, E.C. Confortin, C.D.S. Frank, *CLEAN-Soil, Air, Water*. 37 (2009) 365-371.
- [68] A. Gil, L.A. Galeano, M.Á. Vicente, *Applications of Advanced Oxidation Processes (AOPs) in Drinking Water Treatment*, Cham, Springer International Publishing Springer Nature, 2019.
- [69] S.E. Kariper, *Turkish Computational and Theoretical Chemistry*. 1 (2017) 13-26.
- [70] O.B. Yalcinkaya, A. Yilmaz, B.I. Ceylan, *Chemical Papers*. 74 (2020) 1103-1111.
- [71] D.A. Gálico, R.B. Guerra, A. De Oliveira Legendre, E. Schnitzler, R.A. Mendes, G. Bannach, *Brazilian Journal of Thermal Analysis*. 2 (2013) 45-49.
- [72] V.I. Minkin, *pure and applied*. 71 (1999) 1919-1982.
- [73] C. Matta, R. Gillespie, *Journal of Chemical Education*. 79 (2002) 1141.
- [74] A. Tomberg, gaussian 09w tutorial an introduction to computational chemistry using g09w and avogadro software, p: 14-18.
- [75] T.N. Truong, D.G. Truhlar, *The Journal of chemical physics*. 93(3) (1990) 1761-1769.
- [76] Y. Zhang, G. Zhang, *Chinese Journal of Organic Chemistry*. 34(1) (2014) 178-189.